Expected performance of interferometric air-shower measurements with sparse radio-antenna arrays

Felix Schlüter[a,b,*] **and Tim Huege**[a,c]

[a]*Karlsruher Institut für Technologie, Institut für Astroteilchenphysik, Karlsruhe, Germany*

[b]*Universidad Nacional de San Martín, Instituto de Tecnologías en Detección y Astropartículas, Buenos Aires, Argentina*

[c]*Vrije Universiteit Brussel, Astrophysical Institute, Brussels, Belgium*

E-mail: fschluter@icecube.wisc.edu, tim.huege@kit.edu

Inclined air showers open the window for the radio detection of ultra-high-energy cosmic rays with km-sparse radio-antenna arrays. The potential of those measurements would improve greatly with an accurate reconstruction of the depth of the shower maximum $X_{\max}$. However, traditional methods using the lateral energy fluence distribution at the ground to reconstruct $X_{\max}$ with radio antennas developed for vertical air showers lose their sensitivity. A recently proposed interferometric technique promises measurements of the depth of the shower maximum $X_{\max}$ with an intrinsic accuracy of $3 \, \mathrm{g \, cm^{-2}}$ for very inclined air showers, however, without considering instrumental uncertainties.

In this contribution, we evaluate the potential of interferometric $X_{\max}$ measurements of (simulated) inclined air showers with realistically dimensioned, sparse antenna arrays and account for imperfect time synchronization between individual antennas. We find a strong correlation between the antenna multiplicity (per event) and the maximum acceptable inaccuracy in the time synchronization of individual antennas. We formulate prerequisites for the design of antenna arrays for the application of interferometric measurements: For data recorded with a time synchronization accurate to 1 ns within the commonly used frequency band of 30 MHz to 80 MHz, an antenna multiplicity of $> \sim 50$ is needed to achieve an $X_{\max}$ reconstruction with an accuracy of $20 \, \mathrm{g \, cm^{-2}}$. This multiplicity is achieved by measuring inclined air showers with zenith angles $\theta \geq 77.5°$ with 1 km spaced antenna arrays, while vertical air showers with zenith angles $\theta \leq 40°$ require an antenna spacing below 100 m. Furthermore, we find no improvement in the $X_{\max}$ resolution applying the interferometric reconstruction to simulated radio signals at higher frequencies, i.e., up to several hundred MHz.

---

*Speaker

1. Introduction

The application of interferometric techniques for the detection of extensive air showers induced by ultra-high-energy cosmic rays (UHECRs) carries enormous, so far mostly untouched, potential. While traditional methods only make use of the amplitude information of the radio signal from air showers, interferometric techniques also make use of the shape of the entire waveform which is sensitive to the frequency content and phase of the signal. Thereby, they exploit the coherence between the signals of various detectors, a property unique to the radio emission from air showers.

In this proceeding, we concentrate on the reconstruction of the depth of the shower maximum X_{max} for inclined air showers. X_{max} is widely used to infer the mass of UHECRs, the precise determination of which remains one of the most important challenges in high-energy astroparticle physics today. Inclined air showers are of particular interest for two reasons: First, their large footprint allows their detection with kilometer-sparse radio antenna arrays suitable to detect UHECR at the highest energies [1, 2]. And second, a particle detector can measure the number of muons in inclined air showers (because the electromagnetic particles are absorbed in the atmosphere) which is anti-correlated with X_{max} for different primaries [3]. Hence, a hybrid detector would significantly improve its mass sensitivity. However, the accurate reconstruction of X_{max} from inclined air showers with a (radio) surface detector array has yet to be demonstrated, hence interferometric techniques could, for the first time, enable those hybrid measurements with X_{max} sensitivity.

The technique described and evaluated in this work has been recently proposed in [4, 5]. In this proceeding, we evaluate this technique using realistic assumptions for a sparse antenna array. From this, experimental requirements for the application of this technique can be formulated. Finally, we will discuss which experiments are promising to apply this technique successfully. A more comprehensive discussion of this work, including the reconstruction of the shower axis using interferometry (which is an input to the X_{max} reconstruction), can be found in [6].

We evaluate this technique with air shower simulations tailored to match the ambient conditions present at the Pierre Auger Observatory (observation altitude, magnetic field, atmosphere, ...). The majority of results presented here applies to the radio emission in the 30 MHz to 80 MHz frequency band. The adaptation to other frequency bands is discussed in the end.

2. The method

At the core of this method is the calculation of a beam-formed waveform $B_j(t)$ at an arbitrary point in space $\vec{j}$ using the recorded waveforms at each observer $S_i(t)$ with position $\vec{i}$. For the beam-forming, the light propagation time $\Delta_{i,j}$ between point $\vec{j}$ and every observer position is calculated along straight lines taking into account the speed of light in the atmosphere with a non-unity refractive index

$$\Delta_{i,j} = \frac{d_{i,j} \cdot \overline{n}_{i,j}}{c}, \tag{1}$$

with $d_{i,j}$ and $\overline{n}_{i,j}$ denote the distance and average refractive index between point $\vec{j}$ and an observer at position $\vec{i}$. With that, B_j is determined by the sum of each time-shifted waveform

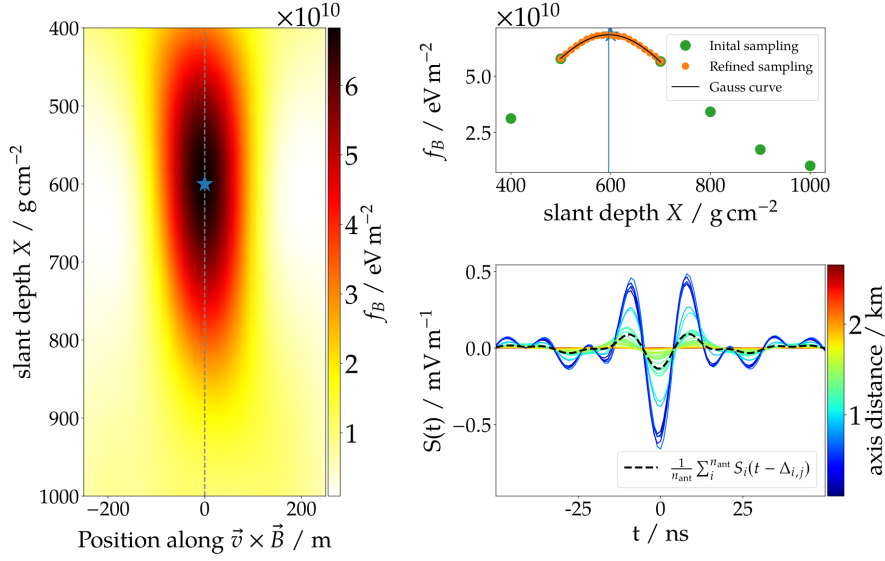$$B_j(t) = \sum_i^N S_i(t - \Delta_{i,j}). \tag{2}$$

Figure 1: *Left*: Cross-section of the longitudinal development of an air shower described by the beam-formed radio signal. The signal is the strongest around the shower axis (dashed vertical line), and the maximum is indicated by a star. *Top-Right*: Longitudinal profile of the beam-formed signal sampled at different depths. *Bottom-Right*: The time-shifted waveforms $S_i(t - \Delta_{i,j})$ (colored) at the location of maximum coherence (star) and the normalized beam-formed waveform (black). The color code shows the lateral axis distance of the observed waveforms.

As waveform $S_i(t)$, we use only the radio emission in the $\vec{v} \times \vec{B}$ polarisation. From the beam-formed waveform we calculate the energy fluence f_{B_j}, see [6, Eq. 3.4]. Other than the bandpass filter, we do not simulate any detector response.

It should be mentioned that in a refractive medium radio emission propagates on curved rays and not, as assumed here, along straight lines. However, in [7] it is shown that this straight-line approximation is sufficient for the emission from very inclined air showers below 100 MHz. Furthermore, for inclined air showers, where the radio emission propagates large distances through the atmosphere, the curvature of the Earth has to be taken into account. That prevents an analytic determination of the average refractive index along a certain path and mandates numerical integration. To accelerate computation we use tables of the average refractive index determined numerically and made public in [8].

Now, to determine X_{max}, we "scan" the atmosphere to find the location at which the coherent emission f_{B_j} is maximum. First, we search for a straight line, i.e., the shower axis, along which f_{B_j} is maximal using a raster search in several 2-dimensional planes which are approximately orthogonal to the shower axis. Then, we sample f_{B_j} along the found axis and determine the maximum with a Gaussian fit. Fig. 1 (*left*) shows a cross-section of f_{B_j}, i.e., a "tomographic map", in a plane defined by the orthogonal axes $\vec{v}$, the direction of the shower, and $\vec{v} \times \vec{B}$ with $\vec{B}$ being the Earth's magnetic field vector. The longitudinal development of the shower is shown along the y-axis in g cm^{-2}, the shower axis is at the center. It is visible, that the coherent emission is strongest at, and around, the shower axis. The top-right panel in the same figure shows the longitudinal profile of the shower (along the shower axis) in f_{B_j}; a maximum is visible. The bottom-right panel shows the time-shifted waveforms
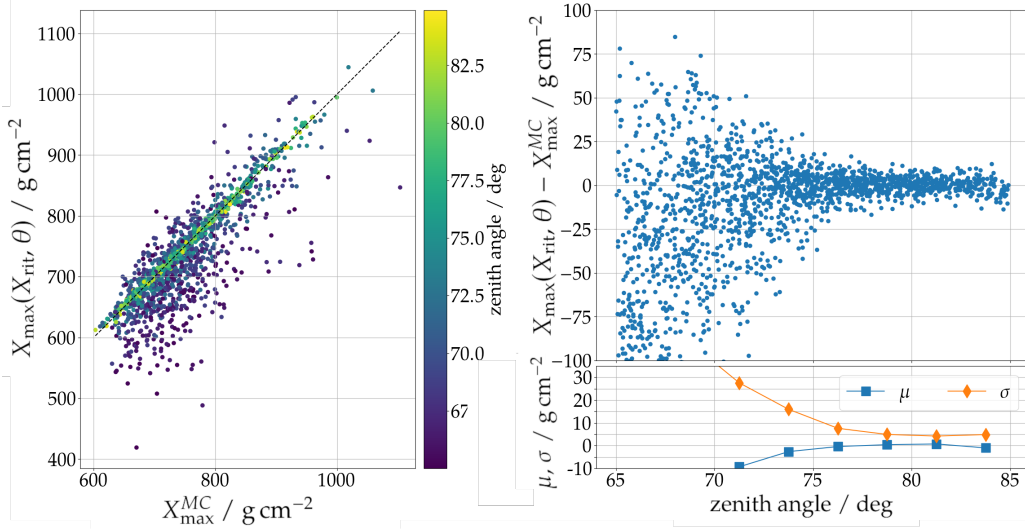
Figure 2: *Left*: Scatter plot of the reconstructed X_{max} as a function of the true X_{max}^{MC}. The color indicates the zenith angle of the individual showers, the dashed line indicates the diagonal along which inclined showers are clustering. *Right*: Residual of the reconstructed shower maximum in $g\,cm^{-2}$ as scatter plot (top) and profile (bottom), i.e., mean and standard deviation, as a function of the zenith angle.

of individual observers together with the beam-formed, normalized waveform for the position at which the coherence is strongest. It was found that the position at which the coherent emission is strongest, described by its slant depth X_{RIT} (RIT stands for Radio-Interferometric-Technique), does not coincide with X_{max} but is linearly correlated with it and thus can be used to reconstruct it [4]. This correlation depends on the zenith angle and, based on our simulations, can be described with:

$$X_{max}(X_{RIT}, \theta) = 1.04 \cdot X_{RIT} + \left(68.31 - \frac{\theta - 77.5°}{0.35°}\right) g\,cm^{-2}. \tag{3}$$

3. Reconstruction with a 1.5 km array

To validate the above-introduced method with a realistic, sparse antenna array, we utilize a set of over 4000 proton- and iron-induced air-shower simulations generated with CORSIKA/CoREAS [9, 10]. For those air showers with zenith angles $\theta \in [65°, 85°]$ and energies $E \in [10^{18.4}, 10^{20.2}]$, the radio emission is simulated for antennas arranged on a hexagonal grid with a spacing of 1.5 km. The entire array covers almost $3000\,km^2$ and matches the shape of the Surface Detector array of the Pierre Auger Observatory. While air showers can be simulated at the edge of the array, around their core is at least one full hexagon of antennas.

Fig. 2 shows the reconstruction of X_{max} for those showers using X_{RIT} and Eq. (3). The left panel shows a scatter plot of the reconstructed X_{max} as a function of the true X_{max}^{MC}. The black dashed line indicates the diagonal and an accurate reconstruction, and the color of the markers indicates the zenith angle of the individual showers. It is apparent that, although the overall scatter is considerable, air showers with a large zenith angle cluster around the diagonal and allow an accurate reconstruction of X_{max}. The residual of the reconstructed X_{max} is shown in the right panels, once as a scatter plot
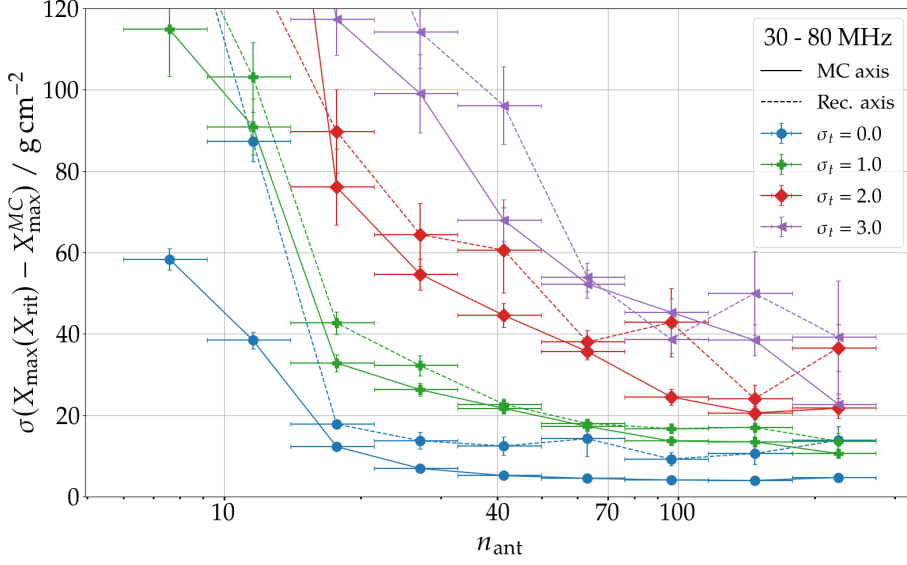
Figure 3: X_{max} resolution as a function of the antenna multiplicity for different time-synchronization scenarios (color-coded) and reconstructed along the true (solid lines) and reconstructed (dashed lines) shower axis.

(*top*) and once only the profile (*bottom*), i.e., mean and standard deviation, as a function of the zenith angle. It can be inferred that an accurate reconstruction is possible for showers above $\sim 75°$. For this reconstruction, perfect time synchronization and perfect knowledge of the shower axis have been assumed. Although an improvement of the X_{max} reconstruction accuracy with the zenith angle has already been reported in [4], the drastic improvements seen here, have to be associated with the increased antenna multiplicity at higher zenith angles as the dominant factor (while the number of antennas was kept constant with a dynamically spaced array in [4]). This relationship, the X_{max} resolution as a function of the antenna multiplicity is shown in Fig. 3. The different colors correspond to different scenarios describing an imperfect time synchronization with a Gaussian time jitter of a certain size which is randomly applied to each signal. Furthermore, we reconstruct X_{max} once along the true, and once along the interferometrically reconstructed shower axis (solid and dashed lines). It can be inferred that, even with perfect time synchronization, a minimum of 15 - 20 stations is required to facilitate an accurate reconstruction with a resolution below $20\,\mathrm{g\,cm^{-2}}$. However, above that value, the resolution does not strongly depend on the antenna multiplicity anymore. With a moderate time jitter of 1 ns more than 50 stations are required for a similar resolution.

It should be stressed that we have not simulated any trigger and hence the treatment in this work resembles an unrealistic trigger-less data taking. With a trigger the number of antennas with recorded data decreases.

4. Interplay between antenna multiplicity and time synchronization for reconstruction resolution

To investigate the interplay of antenna multiplicity and time synchronization on the achievable X_{max} resolution, we use a second set of air shower simulations at a fixed zenith angle of 77.5° but with a very dense antenna array with 250 m spacing. This array comprises on average 1342 antennas.
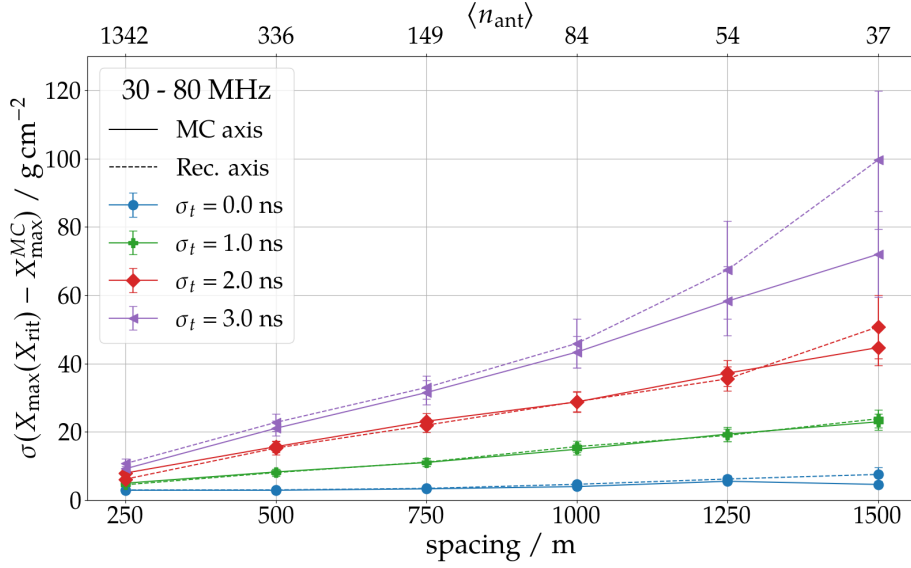
Figure 4: X_{max} resolution for the reconstruction of air showers with a zenith angle of 77.5° with arrays of different antenna spacing (x-axis), i.e., with different antenna multiplicities (upper x-axis), and different assumptions for the time synchronization described by different Gaussian time jitters (color-coded). The solid (dashed) lines indicate the X_{max} reconstruction along the true (a reconstructed) shower axis.

However, from this one can define sub-arrays with larger spacing and fewer antennas, to mimic more sparse arrays measuring the same showers. Fig. 4 shows the X_{max} resolution as a function of the antenna spacing/multiplicity, on the bottom and top x-axis respectively, and for different assumptions for the time synchronization. Two things can be concluded: First, with perfect time synchronization, the antenna multiplicity is in any case sufficient and has no positive effect on the resolution. And second, with imperfect time synchronization, a larger number of antennas mitigates the effect of the imperfect synchronization.

5. Discussion

So far, we have only studied highly inclined air showers. In order to generalize our results to less inclined air showers, we assume that the size of the footprint, and thus the number of triggered antennas, scales with

$$A \sim \frac{\pi r_{che}^2}{\cos \theta}, \tag{4}$$

where r_{che} is the radius of the Cherenkov ring which changes as a function of the zenith angle [6]. Fig. 5 shows the change in footprint size and antenna spacing as a function of the zenith angle. From that, it can be inferred that one needs an antenna spacing of ~ 100 m to measure air showers at 40° with a similar antenna multiplicity and thus X_{max} resolution as at 77.5° with an antenna spacing of 1000 m.

To apply this technique, a multiplicity of at least 15 to 50 triggered antennas per air shower, depending on the achievable timing synchronization, is required. This prerequisite is hardly met by large air shower radio detectors such as the upcoming 3000 km² Radio Detector of the upgraded
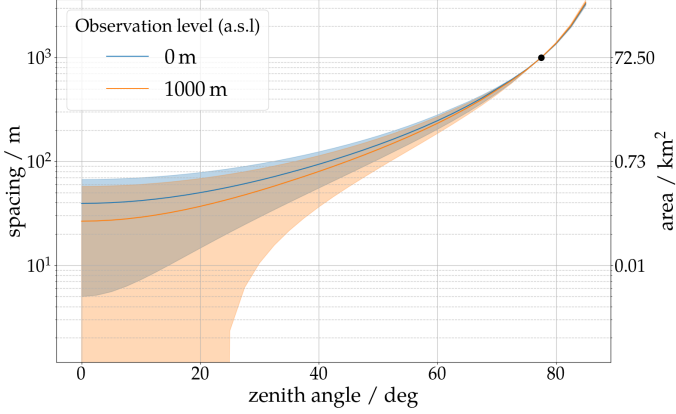
Figure 5: Analytic scaling of the size of the radio-emission-induced footprint as a function of the zenith angle. The left y-axis shows the antenna spacing, and the right y-axis the array size. Along the drawn line the antenna multiplicity is constant. Hence, to archive a comparable resolution as at 77.5° and with 1000 m spacing, at a lower zenith angle, the antenna spacing needs to be reduced according to the black line.

Pierre Auger Observatory [11] or GRAND [12]. The most prominent issue for those experiments is an insufficient GPS-based time synchronization on the level $\gtrsim 5$ ns. The Auger Engineering Radio Array (AERA) uses an external beacon transmitter to improve the GPS-based time synchronization to nanosecond accuracy [13]. However, the asymmetric/irregular array design and the, for inclined air showers, small size of around 17 km^2 (cf. Fig. 5) will reduce the number of suitable showers. Dedicated radio interferometers, which are also used for astronomical measurements, like LOFAR [14], OVRO-LWA [15] or the upcoming Square Kilometer Array [16, 17] are in a unique situation of offering high antenna multiplicity and excellent time synchronization. Thus, those experiments are good candidates to apply and explore interferometric reconstruction algorithms.

Another, yet unexplored opportunity is to measure the "L-parameter" of air showers with this technique [17]. This parameter describes the width of the longitudinal profile of an air shower and can be used to study the mass composition of UHECR and hadronic interaction models at the same time.

So far, we have only applied the method to radio signals between 30 MHz and 80 MHz. However, envisioned air shower radio arrays of IceCube or GRAND aim to utilize higher frequencies. At higher frequencies – we studied two additional frequency bands from 50 MHz to 200 MHz and from 150 MHz to 350 MHz – the strength of the galactic emission diminishes, while close to the Cherenkov ring, the strength of the emission from air showers increases, yielding better signal-to-noise ratios. However, the footprints of the radio emission at higher frequencies also become more "narrow", as most of the signal is accumulated around the Cherenkov ring. Hence, arrays need to be denser to sample this narrow ring sufficiently. It comes as no surprise that measurements at higher frequencies demand a more accurate time synchronization. Besides that we observed two phenomena: First, the fact that only at the Cherenkov ring the emission is strong requires more dense arrays. And second, The observed maximum in the tomographic maps (cf. Fig. 1 *left*) becomes more narrow. Although this in theory allows for a more precise determination of the shower axis and/or X_{max}, it complicates the search for the maximum and increases the chance of miss-identifying a wrong, local maximum.

6. Conclusion

We studied the achievable X_{max} resolution with a novel interferometric reconstruction for realistic air-shower radio arrays. This entails realistic spacing and imperfect time synchronization between the

antennas but no trigger simulation. The maximal tolerable inaccuracy in the time synchronization for an accurate X_{max} reconstruction depends on the number of antennas participating in the reconstruction. For the 30–80 MHz band, an accurate reconstruction of X_{max} ($\sigma_{X_{max}} \lesssim 20 \text{g cm}^{-2}$) is possible with a time synchronization of 1 ns or better and a sufficiently large number of antennas per shower ($\gtrsim 50$). Those requirements are challenging to achieve for sparse arrays with wirelessly communicating detector arrays like the one of the Pierre Auger Observatory or the planned array of GRAND. However, experiments such as the Square Kilometer Array have great potential to exploit interferometric measurements of X_{max}.

We found no improvement in X_{max} accuracy utilizing higher frequencies while at the same time a more accurate time synchronization between antennas is needed. Hence, it is important for future experiments to also encompass the recording of low-frequency signals down to tens of megahertz.

References

[1] T. Huege and A. Haungs, *Radio detection of cosmic rays: present and future*, *JPS Conf. Proc.* **9** (2016) 010018 [1507.07769].

[2] PIERRE AUGER collaboration, *Measurements of Inclined Air Showers with the Auger Engineering Radio Array at the Pierre Auger Observatory*, *PoS* **ICRC2019** (2021) 274.

[3] E.M. Holt et al., *Enhancing the cosmic-ray mass sensitivity of air-shower arrays by combining radio and muon detectors*, *Eur. Phys. J.* **C79** (2019) 371 [1905.01409].

[4] H. Schoorlemmer and W.R.C. Jr, *Radio interferometry applied to the observation of cosmic -ray induced extensive air showers*, 2006.10348.

[5] H. Schoorlemmer and W.R. Carvalho, *Radio interferometry applied to the observation of cosmic -ray induced extensive air showers*, *Eur. Phys. J. C* **81** (2021) 1120 [2006.10348].

[6] F. Schlüter and T. Huege, *Expected performance of air-shower measurements with the radio-interferometric technique*, *JINST* **16** (2021) P07048 [2102.13577].

[7] F. Schlüter et al., *Refractive displacement of the radio-emission footprint of inclined air showers simulated with CoREAS*, *The European Physical Journal C* **80** (2020) .

[8] C. Glaser and F. Schlüter, "A tool package for cosmic-ray and neutrino radio detectors: Tables of integrated refractive index for curved atmospheres." https://github.com/nu-radio/radiotools/blob/master/radiotools/atmosphere/refractivity.py.

[9] D. Heck, J. Knapp, J.N. Capdevielle, G. Schatz and T. Thouw, *CORSIKA: A Monte Carlo Code to Simulate Extensive Air Showers*, FZKA Report 6019, Forschungszentrum Karlsruhe (1998) .

[10] T. Huege, M. Ludwig and C.W. James, *Simulating radio emission from air showers with CoREAS*, *AIP Conf. Proc.* **1535** (2013) 128.

[11] B.P. on behalf of the Pierre Auger Collaboration, *A Large Radio Detector at the Pierre Auger Observatory - Measuring the Properties of Cosmic Rays up to the Highest Energies*, PoS(ICRC2019)395 (2019) .

[12] GRAND collaboration, *The Giant Radio Array for Neutrino Detection (GRAND): Science and Design*, *Sci. China Phys. Mech. Astron.* **63** (2020) 219501 [1810.09994].

[13] PIERRE AUGER collaboration, *Nanosecond-level time synchronization of AERA using a beacon reference transmitter and commercial airplanes*, *EPJ Web Conf.* **135** (2017) 01013 [1609.00630].

[14] P. Schellart et al., *Detecting cosmic rays with the LOFAR radio telescope*, *Astron. Astrophys.* **560** (2013) A98 [1311.1399].

[15] K. Plant et al., *Updates from the OVRO-LWA: Commissioning a Full-Duty-Cycle Radio-Only Cosmic Ray Detector*, *PoS* **ICRC2021** (2021) 204.

[16] T. Huege et al., *Ultimate precision in cosmic-ray radio detection — the SKA*, *EPJ Web Conf.* **135** (2017) 02003 [1608.08869].

[17] S. Buitink et al., *Performance of SKA as an air shower observatory*, *PoS* **ICRC2021** (2021) 415.